Journal of Population Therapeutics & Clinical Pharmacology

CHEMICAL PROCESSES AND UV-C IRRADIATION FOR PHENOL REMOVAL IN INDUSTRIAL WASTE STREAMS

Sumaiya Azam[1], Nabeela Kanwal[2], Anirudh Gupta[3], Dr. Shayan Zufishan[5], Dr. Syeda Asiya Parveen[6], Ali Imran Mallhi[7]

[1]School of Interdisciplinary Engineering and sciences (SINES), National University of Sciences and Technology (NUST), Pakistan, Email: Sumaiyaazam571@gmail.com

[2]Student, Department of Chemistry, The University of Lahore Sargodha Campus, Pakistan, Email: nabeelakanwal615@gmail.com

[3]Assistant Professor, Department of Biotechnology, NIMS Institute of Allied Medical Science and Technology, NIMS University Rajasthan, India, Email: anirudh.gupta2020@gmail.com

[5]Assistant Professor, Department of Biochemistry, Karachi Medical and Dental College, Email: drshayankhan@hotmail.com

[6]Associate Professor, Head of Department, Department of Biochemistry, Karachi Medical and Dental College, Email: doctorasiya@yahoo.com

[7]Assistant Professor, Department of Chemistry, Superior University Faisalabad Campus, Pakistan, Email: imranmallhi72@gmail.com

ABSTRACT:

Background: Industrial processes generate substantial amounts of complex waste materials, necessitating the removal of contaminants before disposal. Phenolic compounds, particularly concerning due to their harmful effects on human health and the environment, are prevalent byproducts in various industrial activities, such as gasoline processing.

Objective: This study aims to investigate the primary factors influencing the reduction of phenolic compounds and their conversion into minerals through chemical processes.

Methods: The original waste discharge, characterized by a pH of approximately 7, containing 5 g L-1 of sand (containing TiO2) and 22 mg L-1 of oxidizing hydrogen peroxide. The reduction process was monitored over 60 minutes, during which the total phenol content decreased by approximately 90%. Phenol levels were measured using an ultraviolet spectrophotometer employing the standard 4-amino antipyrine method at a wavelength of 510 nm. Reactions took place in a reactor equipped with a 95 W UV-C lamp for sterilization.

Results: The reduction process achieved a substantial decrease in phenol content within the specified timeframe. The use of UV-C light facilitated efficient degradation, leading to a notable reduction in phenolic compounds.

Conclusion: Understanding the factors influencing phenol reduction in industrial waste is crucial for effective waste management strategies. This study highlights the efficacy of chemical processes coupled with UV-C irradiation in mitigating phenol pollution, offering a promising approach for environmental remediation efforts.

KEYWORDS: Sand, Organic Molecules, Catalysts, and Petrochemical Waste.

INTRODUCTION:

Industrial processes make a lot of wastewater that must be cleaned before it can be released into the environment. Different types of effluent treatment are being developed and improved to reduce the pollution these compounds cause when they get into large amounts of water. This protects natural resources, human health, and the balance of aquatic environments and ensures that current rules are followed (Pan et al., 2024; Zhao, Kondo, Kuwahara, Mori, & Yamashita, 2024).

Oil production needs to meet these environmental rules right away. Among these parts that come from petrochemical waste and are hard to break down, phenolic chemicals stand out. Things that contain phenol can cause cancer, mutations, and birth defects in unborn babies. They can also be harmful to living things. The Pakistan Environmental Protection Agency has considered phenol a priority organic pollutant (POP) since 1976 (Kim, Jaffari, Abbas, Chowdhury, & Cho, 2024).

Federal law sets a maximum of 0.5 mg L-1 for direct or indirect release into a receiving body (CONAMA n. 430/2011). After the first step, bacterial treatment is one of the most cost-effective ways to treat water effluents. However, using living things to clean up petrochemical waste is a lot trickier than using living things to clean up home or other industrial waste. The bacteria that have been changed are very good at breaking down phenolic chemicals, but they stop cells from growing (He, Yin, Yuan, & Zhang, 2024; Jabbar et al., 2024).

It greatly lowers the biomass's ability to break down when it's in high quantity. In this situation, advanced oxidative processes (AOPs) come into play. These processes change many complex chemical compounds into products easier for living things to break down. It depends on the physical state of the reaction catalyst and whether the POA reaction is homogeneous or heterogeneous (Ren, Zhou, Hu, Chen, & Wang, 2024; Xiao Zhou et al., 2024).

In the last few decades, many researchers and people who design treatment plants have thought that this treatment for phenol was very effective because it breaks down organic

molecules very well, creating low-toxicity intermediate compounds or mineralization with the creation of carbon dioxide, water, and inorganic ions. This study aimed to look into photodegradation to treat petrochemical waste to eliminate phenolic compounds or turn them into minerals. It was also essential to see how pH levels, sand with TiO2 (a natural catalyst), and H2O2 (30% W/V) affected this reaction (J. Chen et al., 2024; L. Zhang et al., 2024).

MATERIAL AND METHODS:

PETROCHEMICAL EFFLUENT COLLECTION:

We took wastewater samples at the air-dissolved floater (FAD) outlet of the Riograndense oil plant (Rio Grande/RS), as seen in Figure 1. The samples were kept in a bottle of amber for about two months under a cold bed at four °C (Zhang, Liu, Tan, & Yu, 2024).

Figure 1 – Dissolved air float at the Riograndense oil refinery.

In Figure 1, you can see dissolved air float at the Riograndense oil plant.

The effluent properties may differ based on the type of oil processing, how the plant is set up, or how it is run. The data on the characteristics of the effluents came from the Refinaria de Petróleo Riograndense. Table 1 shows the total data for the last three months 2018 (Raziq et al., 2024).

PHYSICOCHEMICAL	MEAN CONCENTRATION ± MEAN

COMPOSITION	DEVIATION*
Phenol	12.59 ± 2.58 mg L-1
Nitrate	0.21 ± 0.94 mg L-1
Ammoniacal Nitrogen	13.58 ± 2.57 mg L-1
Mineral Oils and Greases	0.3 ± 0.06 mg L-1
pH	7.38 ± 0.51
Surfactants	0.43 ± 0.11 mg L-1
Nitrite	0.0011 ± 0.0009 mg L-1
COD	390.12 ± 63.67 mg O2 L-1

Table 1 – Physico-chemical characterization of the FAD discharge effluent.

PHOTOCATALYTIC REACTION:

It was done in homogeneous and heterogeneous photodegradation processes to find the best conditions for breaking down phenols. So, an experiment plan was made to see how the heterogeneous catalyst, the concentration of the homogeneous oxidant, and the sample pH affected each other (Fang et al., 2024; Yu et al., 2024).

A 23-factorial design alongside three centre points was used to find the best conditions for the photocatalysis process. Of the 11 tests, the effect of the independent factors on the dependent variable on total phenol degradation (%) was examined. The experimental planning grid can be seen in Table 2 (Cheng et al., 2024; Kamogawa et al., 2024).

TEST	SAND CONCENTRATION(G L^{-1})	OXIDANT CONCENTRATION (MG L^{-1})	pH
1.	0 (5)	0 (22)	0 (7)
2.	+1 (10)	+1 (44)	-1 (4)

3.	-1 (0)	-1 (0)	+1 (10)
4.	+1 (10)	-1 (0)	-1 (4)
5.	-1 (0)	+1 (44)	+1 (10)
6.	0 (5)	0 (22)	0 (7)
7.	0 (5)	0 (22)	0 (7)
8.	+1 (10)	-1 (0)	+1 (10)
9.	0 (5)	0 (22)	0 (7)
10.	+1 (10)	-1 (0)	+1 (10)
11.	-1 (0)	+1 (44)	-1 (4)

Table 2 – Experimental planning matrix with encoded and actual variables.

Each planned test was done in a reactor utilizing a 95W UV-C lamp for an hour. Natural sand with TiO2 was used as a catalyst, and H2O2 (30% W/V) was used as an oxidizer. After that, samples were prepared so the 4-amino antipyrine colourimetric technique, explained in APHA (2012), could measure the total amount of phenolics. Equation 1 can determine the decline (Yan et al., 2024; Zhou, Chen, Li, Chen, & Zhu, 2024).

D = 100-[(Cam*100)/Cb]

About what:

D: total phenolic degradation (%)

Cam: total concentration of phenol in the sample after the reaction (mg L-1)

Cb: total phenol concentration in the raw effluent (mg L-1) (Jian et al., 2024).

RESULTS AND DISCUSSION:

These three factors, sand concentration and H2O2 concentration, were used to study how they affected the total phenolic content in the effluent (the dependent variable). The study used a factorial design of experimentation with three copies of the centre point. Table 3 shows the 2^3 schedule with three central points and the data for each (Q. Chen et al., 2024; Salaverri, Alemán, & Marzo, 2024).

TEST	H_2O_2 CONCENTRATION (MG L^{-1})	SAND CONCENTRATION (G L^{-1})	DEGRADATION (%)	pH
1.	44	0	92.5	4
2.	44	10	92.3	4
3.	0	0	52.0	10
4.	0	10	44.1	10
5.	44	0	76.5	10
6.	44	10	90.0	10
7.	22	5	88.3	7
8.	22	5	89.8	7
9.	22	5	90.8	7
10.	10	0	4	51.1
11.	0	0	4	53.9

Table 3 – Results of planning tests on the total degradation of phenolics in raw effluents.

Statistical methods were used to process the data. The study's results can be seen in Table 4. The concentration of H2O2 is the only parameter with a statistically significant influence on photodegradation at the 95% significance level (Xu et al., 2024).

Interaction	Estimated Effect	Standard Error	P	t-student	Significance Level (+95%)	Significance Level (-95%)
H_2O_2 concentration	37.54	11.05	0.03	3.39	68.22	6.85

(mg L-1) (L)*						
Catalyst concentration (g L-1) (L)	0.64	11.05	0.96	0.06	31.33	-30.04
1L x 3L	2.13	11.05	0.86	0.19	32.81	-28.56
1L x 2L	5.99	11.05	0.62	0.54	36.67	-24.70
2L x 3L	-2.37	11.05	0.84	-0.21	28.32	-33.05
pH (L)	-6.83	11.05	0.57	-0.62	23.85	-37.52
* Significant effect $p<0.05$						

Table 4 shows the estimated effects of factors and statistical analysis factors where the R2 value is 0.99.

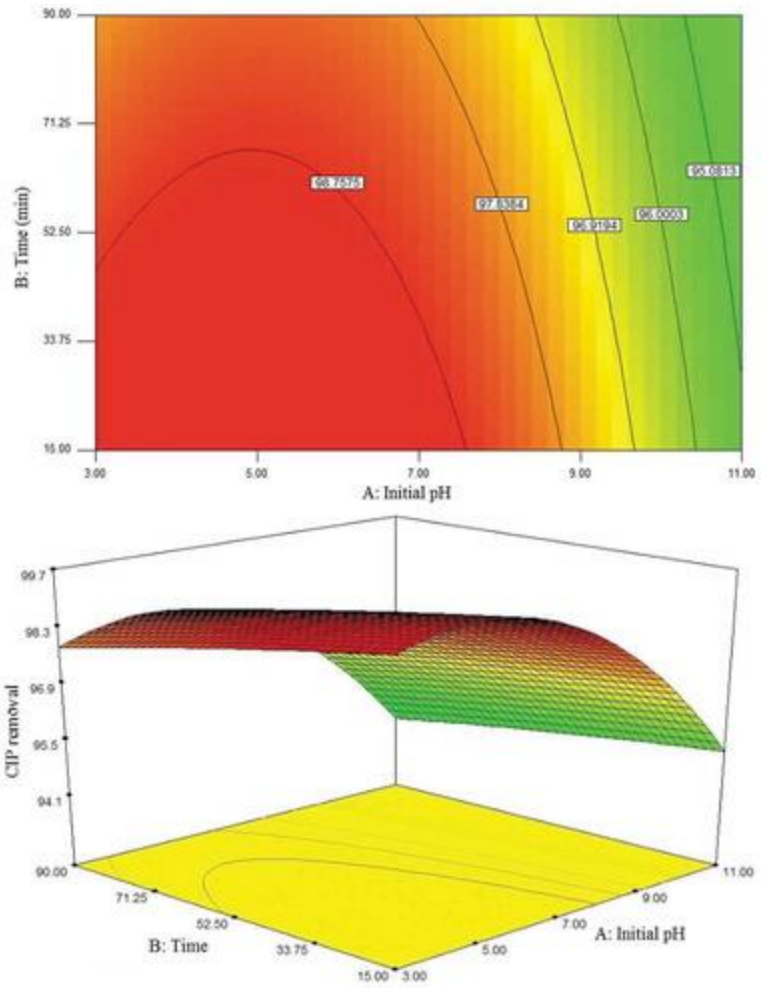

Figure 2: Analysis response profile of sand concentration and hydrogen peroxide concentration variables at pH 7 (raw effluent condition).

This was true for all the concentrations of sand (0–10 g L-1) and H_2O_2 (0–44 mg L-1).

In Figure 2, you can see the impact profile of the factors and percentage and concentration of hydrogen peroxide at pH 7 (raw effluent mode) (Li et al., 2024).

Based on how the experiment was planned, the amount of sand had a negligible effect on the measured time. However, this variable controls the number of free sites of activity on the catalyst TiO2 and the production of hydroxyl radicals. Turbidity can happen when there is a lot of sand within the system. This makes it hard for light to get to the sites and turn them on. When H2O2 is used as an oxidant, it raises the original concentration of hydroxyl radicals (Yang et al., 2024; S. Zhao et al., 2024; J. Zhou et al., 2024).

This differs from solid catalysts, which need UV light to activate the sites and create hydroxyl radicals on the surface. Also, it was seen that the pH level in the range that was tested

didn't make a big difference. The effluent can be used as is without going through an acidification as well as alkalinization phase (Wang & Zhang, 2024).

CONCLUSION:

Photocatalytic reactions can break down the phenolic chemicals found in petrochemical waste, which can also be used before biological treatment.

The reaction between 5 g L-1 of sand as well as 22 mg L-1 of H2O2 30% W/V and raw sewage with a pH of 7 broke down 89.6% (±0.9) of the total amount of phenol in 60 minutes, without the need for any acidification or alkalization steps. Because of this, the photodegradation process worked well and quickly in the given situation.

REFERENCES:

1. Chen, J., Li, M., Yang, Y., Liu, H., Zhao, B., Ozaki, Y., & Song, W. (2024). In-situ surface-enhanced Raman spectroscopy reveals metal–organic frameworks' role in photocatalytic reaction selectivity on susceptible and durable Cu-CuBr substrate. *Journal of Colloid and Interface Science, 660*, 669-680.
2. Chen, Q., Ning, C., Fang, J., Ping, B., Li, G., Kong, L., . . . Ruan, Q. (2024). Redirecting the electron flow to coordinate oxidation and reduction reactions for efficient photocatalytic H2O2 production. *Chemical Engineering Journal*, 150581.
3. Cheng, J., Wu, Y., Zhang, W., Zhang, J., Wang, L., Zhou, M., . . . Xu, H. (2024). Fully Conjugated 2D sp2 Carbon-Linked Covalent Organic Frameworks for Photocatalytic Overall Water Splitting. *Advanced Materials, 36*(6), 2305313.
4. Fang, R., Yang, Z., Sun, J., Zhu, C., Chen, Y., Wang, Z., & Xue, C. (2024). Synergistic mediation of dual donor levels in CNS/BOCB-OV heterojunctions for enhanced photocatalytic CO 2 reduction. *Journal of Materials Chemistry A, 12*(6), 3398-3410.
5. He, Y., Yin, L., Yuan, N., & Zhang, G. (2024). Adsorption and activation, active site and reaction pathway of photocatalytic CO2 reduction: A review. *Chemical Engineering Journal*, 148754.
6. Jabbar, Z. H., Graimed, B. H., Okab, A. A., Ammar, S. H., Najim, A. A., Radeef, A. Y., & Taher, A. G. (2024). Preparation of magnetic Fe3O4/g-C3N4 nanosheets immobilized with hierarchal Bi2WO6 for boosted photocatalytic reaction towards antibiotics in aqueous solution: S-type charge migration route. *Diamond and Related Materials, 142*, 110817.

7. Jian, L., Dong, Y., Zhao, H., Pan, C., Wang, G., & Zhu, Y. (2024). Highly crystalline carbon nitrogen polymer with a strong built-in electric fields for ultra-high photocatalytic H2O2 production. *Applied Catalysis B: Environmental*, *342*, 123340.
8. Kamogawa, K., Kato, Y., Tamaki, Y., Noguchi, T., Nozaki, K., Nakagawa, T., & Ishitani, O. (2024). Overall reaction mechanism of photocatalytic CO 2 reduction on a Re (i)-complex catalyst unit of a Ru (ii)–Re (i) supramolecular photocatalyst. *Chemical Science*, *15*(6), 2074-2088.
9. Kim, C.-M., Jaffari, Z. H., Abbas, A., Chowdhury, M. F., & Cho, K. H. (2024). Machine learning analysis to interpret the effect of the photocatalytic reaction rate constant (k) of semiconductor-based photocatalysts on dye removal. *Journal of Hazardous Materials*, *465*, 132995.
10. Li, P., Wang, Y., Wang, J., Wang, W., Ding, Z., Liang, J., & Fan, Q. (2024). The photocatalytic oxidation of As (III) on birnessite. *npj Clean Water*, *7*(1), 19.
11. Pan, Y., Abazari, R., Tahir, B., Sanati, S., Zheng, Y., Tahir, M., & Gao, J. (2024). Iron-based metal–organic frameworks and their derived materials for photocatalytic and photoelectrocatalytic reactions. *Coordination Chemistry Reviews*, *499*, 215538.
12. Raziq, F., Rahman, M. Z., Ali, S., Ali, R., Ali, S., Zada, A., . . . Qiao, L. (2024). Enhancing Z-scheme photocatalytic CO2 methanation at extended visible light (> 600 nm): Insight into charge transport and surface catalytic reaction mechanisms. *Chemical Engineering Journal*, *479*, 147712.
13. Ren, G., Zhou, M., Hu, P., Chen, J.-F., & Wang, H. (2024). Bubble-water/catalyst triphase interface microenvironment accelerates photocatalytic OER via optimizing semi-hydrophobic OH radical. *Nature communications*, *15*(1), 2346.
14. Salaverri, N., Alemán, J., & Marzo, L. (2024). Harnessing the Power of the De Mayo Reaction: Unveiling a Photochemical and Photocatalytic Masked [2+ 2] Methodology for Organic Synthesis. *Advanced Synthesis & Catalysis*, *366*(2), 156-167.
15. Wang, J., & Zhang, D. (2024). Insights into atom-level local reactions for CO2 photocatalytic production: Reaction pathways and product selectivity at the atomic level. *Journal of Cleaner Production*, 141676.

16. Xu, Q., Wu, J., Qian, Y., Chen, X., Han, Y., Zeng, X., . . . Zhu, Q. (2024). Order–Disorder Engineering of Carbon Nitride for Photocatalytic H2O2 Generation Coupled with Pollutant Removal. *ACS Applied Materials & Interfaces, 16*(1), 784-794.
17. Yan, Y., Gu, X., Zheng, S., Zhang, J., Xia, S., & Li, F. (2024). Designing a type II heterojunction ZnFe2O4/ZnGa2O4 for photocatalytic reaction: Theoretical investigation. *International Journal of Hydrogen Energy, 59*, 224-233.
18. Yang, J., Liu, B., Zeng, L., Du, B., Zhou, Y., Tao, H., . . . Zhu, M. (2024). Confining Bismuth-Halide Perovskite in Mesochannels of Silica Nanomembranes for Exceptional Photocatalytic Abatement of Air Pollutants. *Angewandte Chemie*, e202319741.
19. Yu, C., Jin, J., Yan, H., Zhou, G., Xu, Y., Tang, L., . . . Lu, Z. (2024). Spaced double hydrogen bonding for highly efficient and selective photocatalytic air reductive H2O2 synthesis. *Angewandte Chemie*, e202400857.
20. Zhang, G., Liu, J., Tan, Z., & Yu, H. (2024). Multivariate modeling of intrinsic kinetics for gas-solid heterogeneous photocatalytic reaction: A general method for different pollutant-photocatalyst systems. *Chemical Engineering Journal, 479*, 147651.
21. Zhang, L., Li, R.-H., Li, X.-X., Wang, S., Liu, J., Hong, X.-X., . . . Lan, Y.-Q. (2024). Photocatalytic aerobic oxidation of C (sp3)-H bonds. *Nature communications, 15*(1), 537.
22. Zhao, S., Zhang, C., Wang, S., Lu, K., Wang, B., Huang, J., . . . Liu, M. (2024). Photothermally driven decoupling of gas evolution at the solid–liquid interface for boosted photocatalytic hydrogen production. *Nanoscale, 16*(1), 152-162.
23. Zhao, Y., Kondo, Y., Kuwahara, Y., Mori, K., & Yamashita, H. (2024). Two-Phase Reaction System for Efficient Photocatalytic Production of Hydrogen Peroxide. *Applied Catalysis B: Environment and Energy*, 123945.
24. Zhou, J., Zha, X., Chen, Z., Li, K., Sun, H., Wang, J., . . . Zhao, Z. (2024). Tailoring the coordination microenvironment of single-atom W for efficient photocatalytic CO2 reduction. *Applied Catalysis B: Environment and Energy*, 123911.
25. Zhou, X., Chen, D., Li, T., Chen, X., & Zhu, L. (2024). Pd and carbon quantum dots co-decorated TiO2 nanosheets for enhanced photocatalytic H2 production and reaction mechanism. *International Journal of Hydrogen Energy, 53*, 1361-1372.

26. Zhou, X., Tian, L., Wu, H., Chen, X., Zhang, J., Li, W., . . . Liu, Y. (2024). Reusable and self-sterilization mask for real-time personal protection based on sunlight-driven photocatalytic reaction. *Journal of Hazardous Materials, 466,* 133513.